

Synchrotron Light on Ribosomes: The Development of Crystallographic Studies of Bacterial Ribosomal Particles

Klaus S. Bartels¹, Gabriela Weber¹, Shulamit Weinstein², Heinz-Günter Wittmann³, and Ada Yonath^{1,2}

Table of Contents

1 Introduction	58
2 From "Powder" Samples to Single Crystals — Some History	58
2.1 <i>E. coli</i> and <i>B. Stearothermophilus</i>	58
2.2 <i>Halobacterium Marismortui</i>	63
3 Crystallographic Data Collection — Recent Developments	64
3.1 <i>Bacillus Stearothermophilus</i>	64
3.2 <i>Halobacterium Marismortui</i>	65
4 Phase Determination	68
5 Summary	71
6 Acknowledgements	71
7 References	71

¹ Max-Planck-Arbeitsgruppen für strukturelle Molekularbiologie, c/o DESY, Notkestr. 85, D-2000 Hamburg 52

² Weizmann Institute of Science, Rehovot, Israel

³ Max-Planck-Institut für molekulare Genetik, Ihnestr. 73, D-1000 Berlin 33

1 Introduction

If ever a desperate project benefited from the availability of synchrotron radiation, that project is the crystallographic study of ribosomal particles.

Ribosomes are unique assemblies of several strands of RNA and of a large number of different proteins, representing the living cell's protein factory. Upon initiation of the biosynthetic process, one larger and one smaller subunit associate to form the active cell organelle that reads genetic information from the messenger RNA and translates it into a specific polypeptide chain. To this end, several binding sites are provided: for the messenger, for the tRNAs carrying the amino acids, for GTP, and a variety of other factors.

The large subunit of a typical eubacterial ribosome (MW ca. 1,600,000) is composed of 2 RNA chains and about 35 different proteins, the small subunit (MW ca. 700,000) comprises 1 RNA chain and about 21 proteins.

The chemical and physical properties of ribosomes are well characterized (for reviews see ¹⁻⁵). The exact understanding of their function, however, still lacks a detailed molecular model. Appropriate methods such as image reconstruction from electron micrographs of two-dimensional sheets, or X-ray structure analysis, all depend on the crystallizability of the material.

Experiments towards growing ribosomal crystals *in vitro* were challenged by the observations that ribosomes may self-organize into ordered aggregates in the living cell; two-dimensional arrays have been found under special conditions, such as hibernation or lack of oxygen (e.g. ⁶⁻⁸). However, the complex structure, the enormous size and the flexibility of ribosomal particles render their crystallization *in vitro* extremely difficult. Therefore, only a few successful efforts to produce three-dimensional crystals have been reported (e.g. ⁹⁻¹¹).

2 From "Powder" Samples to Single Crystals — Some History

For a number of years now we have been involved in crystallization of bacterial ribosomal particles. From the very beginning of our studies, the crucial need for a stable, very intense, and perfectly focussed synchrotron beam was evident, even for preliminary and basic information (e.g. whether crystals diffract at all). Thus our studies have always been dependent on the availability of synchrotron beam time and hampered by only partial (and very occasional) feedback to assess our experimental procedures for growing bacteria, preparing the ribosomes and obtaining crystals.

2.1 *E. coli* and *B. Stearothermophilus*

Our first microcrystals were of *Bacillus stearothermophilus* 50S subunits ⁹) and of 70S ribosomes from *E. coli* ¹²); they were mainly grown from lower alcohols, toluene, or chloroform. Each ribosomal preparation required slightly different crystallization conditions, and often the preparation had almost been exhausted by the time conditions were optimised. We also found that crystals grew from active particles only.

Every step in our crystallization experiments was checked carefully with electron microscopy and a high magnification light microscope ($100\times$ and more); lower magnification would often not reveal the minute first signs of success.

Large amounts of microcrystals from *B. stearothermophilus* 50S subunits were collected in X-ray capillaries (and even larger amounts were lost during this procedure), centrifuged to achieve dense packing, and carried to the X-ray beam. Imagine the atmosphere of a synchrotron concrete bunker and the excitement in the middle of the night, when — for the first time — the small-angle X-ray photograph of a supposed suspension of microcrystals really showed Debye-Scherrer diffraction rings of a “powder” sample, albeit at very low Bragg resolution!

This stage of our studies can be described as endless attempts to obtain meaningful diffraction patterns. High angle diffraction photographs would occasionally show weak but sharp rings (Fig. 1a), some of them with spacings similar to those that were previously reported for gels of ribosomes and extracted rRNA (e.g. 10.4 \AA , 7.8 \AA , 5.6 \AA , 4.9 \AA , and 3.4 \AA ; cf. ¹³⁻¹⁵).

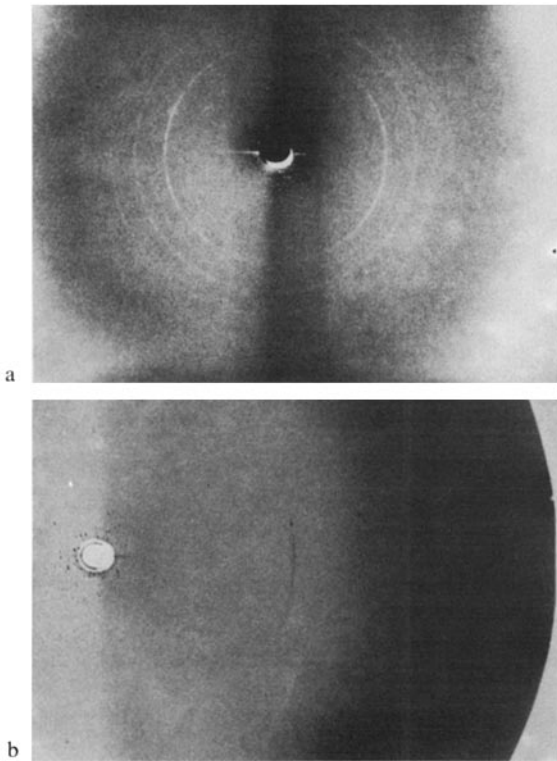


Fig. 1a and b. Early diffraction patterns (obtained at X11/EMBL/DESY) show few reflexion spots from microcrystals and fiber diffraction from the RNA moiety. **a** Unordered crystals; several full rings with spacings that arise from RNA; **b** partly ordered crystals, as described in the text, two arcs of fiber diffraction

Later on we succeeded in partially aligning microcrystals within the sample: they were placed in X-ray capillaries and pulled down by gently sucking their mother liquor, whereupon the needle-shaped crystals oriented along the capillary axis. Such samples sometimes, but only under perfect measuring conditions, produced pseudo fiber patterns which consisted of oriented arcs with average length of 60° (Fig. 1b). In many cases these arcs were composed of distinct spots that could be clearly resolved by eye. Since such patterns may arise from partial orientation of the nucleic acid component within fairly well packed particles, these patterns indicated reasonable internal order.

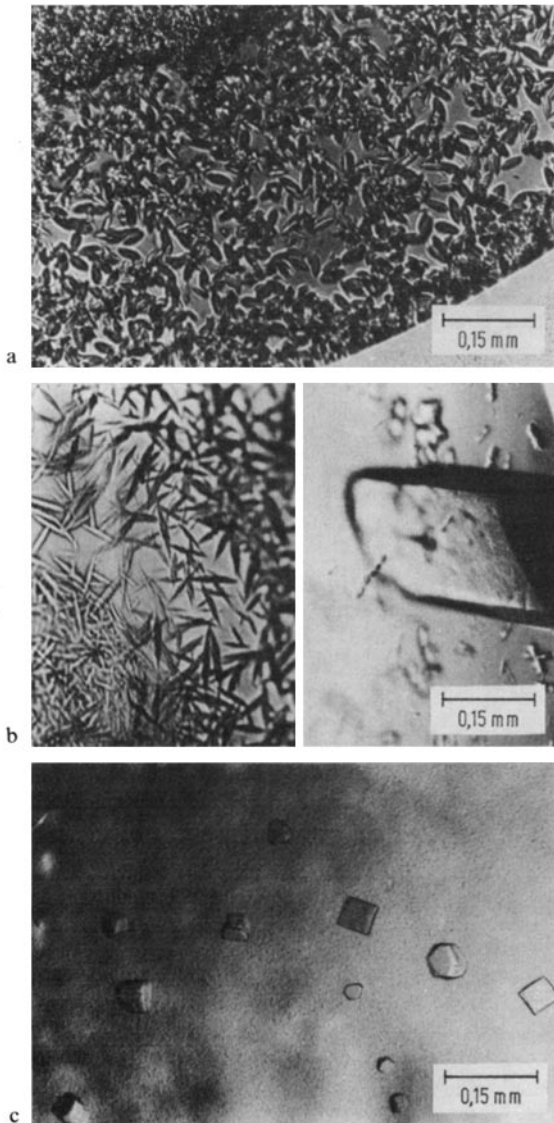


Fig. 2a-c. Different crystal forms of *B. stearothermophilus* 50S subunits (bar length 0.15 mm) **a** grown from 10% toluene, 0.5M NaCl at pH 6.2 (MES-buffer); **b** grown from 2.5% PEG 6000, 0.18M ammonium sulfate, 0.03M $MgCl_2$, and 0.09M KCl at pH 6.4 (MES-buffer) (left) and grown from 2.5% PEG 6000, 0.18M ammonium sulfate, 0.03M $MgCl_2$, and 0.54M KCl at pH = 6.6 (MES-buffer) (right); **c** grown from 2.5% PEG 6000, 0.015M ammonium sulfate, and 0.02M $MgCl_2$ at pH 6.4 (MES-buffer)

In favourable cases larger (though still tiny) crystals produced the first X-ray patterns on which distinct reflexions with periodic spacings could be detected (Fig. 1), thus encouraging further efforts.

Increasing the size of the crystals as well as their internal order by slowing down the crystallization process failed, probably because of deterioration of the particles before they could form aggregates; the latter seem to play an essential role in the nucleation process ¹⁶⁾.



Fig. 3. Crystals of *B. stearothermophilus* 50S subunits grown in X-ray capillaries from methanol/ethylene glycol (at pH 8.4). Cracks develop within a few hours after sealing the capillaries ²⁰⁾ (bar length = 0.15 mm)

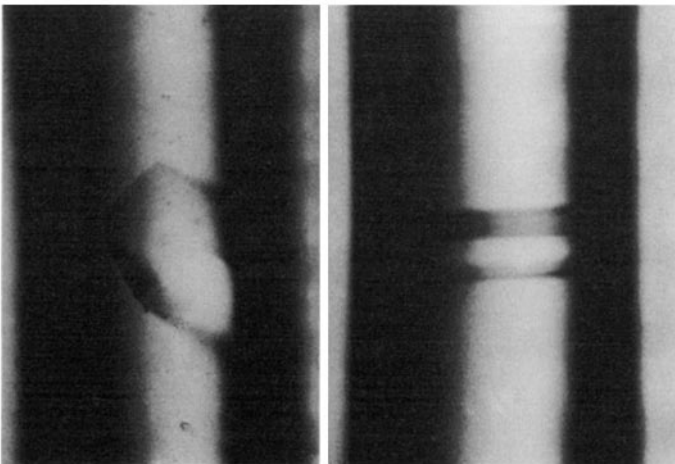


Fig. 4. *B. stearothermophilus* 50S needles grow mostly along the capillary axis but some of them also grow in different directions ²⁰⁾ (same conditions as in Fig. 3; capillary diameter = 0.7 mm)

A systematic exploration of parameters influencing crystal growth in ribosomal systems, and a fine control of the volume of the crystallization droplet by balancing water and alcohol diffusion through addition of salt to the reservoir¹⁷⁾, eventually led to a number of different crystal forms for *B. stearothermophilus* 50S subunits (Figs. 2–4; cf. ^{18–22)}). Long pointed needles of up to 1.5 mm length grew directly in X-ray capillaries by vapor diffusion of alcohol mixtures. These crystals were stable for three to five months when kept in their natural growth medium at 4 to 7 °C.

Since precipitants used for growth were volatile alcohols (methanol, or methanol/ ethylen glycol mixtures) any handling of the crystals was impossible. Even a minor intervention such as sealing the X-ray capillaries shortened the lifetime of crystals drastically to 6–8 hours (Fig. 3); crystals had to be irradiated immediately in their original growth solution.

Most of the crystals grew with their long axis parallel to the capillary axis, but a fair number of them grew in different directions (Fig. 4). Thus we were able to obtain diffraction patterns from all of the crystallographic zones without manipulating the crystals^{20, 21)} (Fig. 5), despite the natural overcrowding of crystals which often imposes difficulties in finding solitary crystals in proper orientations (Fig. 5c).

All patterns showed a sharp decay in intensities at about 20 to 22 Å. Thus we were misled into believing that 20 Å was the actual resolution limit. Only much later, when crystals grew larger and measuring facilities were further improved, did we discover that the crystals are ordered internally to much higher level, close to that indicated by the “powder” diffraction.

Since we had to irradiate crystals within their growth solution in their original orientation, and at the same time to avoid other crystals in close proximity, we were strongly dependent not only on the intensity and the stability, but also on the size and shape of the incident beam. As a consequence, improvements in the quality of the data collection facilities were needed, alongside our efforts to improve the crystal quality.

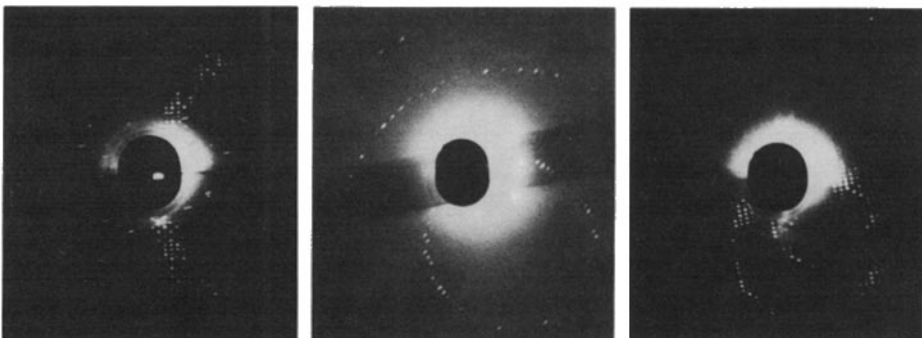


Fig. 5a–c. Diffraction patterns (obtained at 9.6/SRS/Daresbury and A1/CHESS/Cornell U.) from crystals like those in Fig. 4, exposed at -2 °C. **a** The twofold screw axis $c = 905$ Å can be seen on the edge of the $0k1$ -lune; rotation range 0.8° . Spurious streak-like reflexions result from neighbouring crystals in the capillary. **b** Still photograph close to the (tilted) $hk0$ -orientation, $a = 350$ Å, $b = 670$ Å. **c** This picture demonstrates the difficulty in selecting a single crystal within the cross section of the X-ray beam

Among other developments, a new collimator system composed of two double slits was designed and built at EMBL/DESY ²³⁾. Using the double focussing X-ray EMBL instruments equipped with this collimator system, we obtained sharp, resolvable patterns with enhanced signal to noise ratio, and we were able to determine cell dimensions ²¹⁾.

2.2 Halobacterium Marismortui

Bearing in mind the technical difficulties arising from volatile organic solvents as precipitants, we also looked for ribosomes that are stable under high salt concentrations; they could perhaps be crystallized using “conventional” precipitants such as ammonium sulfate or other non-volatile agents. Thus the crystals could be handled with less difficulties and mounted in the conventional way in X-ray capillaries.

Ribosomes from halophilic bacteria meet this requirement; furthermore, the structure of a ribosome of an archaeobacterium (*Halobacterium marismortui*) as compared to that of a eubacterium (*Bacillus stearothermophilus*) might prove a valuable extension of our studies.

The first microcrystals of *H. marismortui* 50S subunits were obtained at 4 °C from PEG in growth solutions that mimic the natural environment within these bacteria: Potassium, ammonium, magnesium and chloride ions were present in the crystallization solution at the minimum concentrations needed for reserving their activity ²⁴⁾.

Later on, advantage was taken of the delicate equilibrium of mono- and divalent ions needed for the growth of halobacteria. Crystals then grew at the minimum concentration of salts needed for storage without activity loss. They appeared as thin plates with dimensions of about $0.4 \times 0.4 \times 0.1$ mm at 19 °C, but tended to form multilayer aggregates ²⁵⁾ (Fig. 6). Their X-ray diffraction patterns extended to about 13 Å resolution.



Fig. 6. Thin plates of *H. marismortui* 50S subunits grow spontaneously from PEG in the presence of salts (KCl) in hanging drops but tend to form multilayer aggregates ²⁵⁾ (bar length = 0.15 mm)

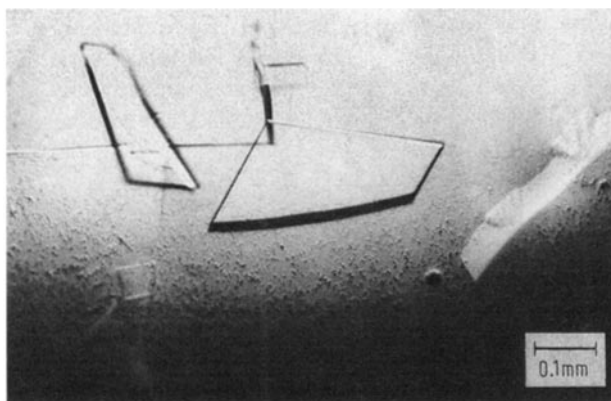


Fig. 7. Crystals of *H. marismortui* 50S subunits grown after seeding²⁷⁾. The face displays the monoclinic angle of 71° of the reduced cell (bar length = 0.1 mm)

It was found for spontaneous crystal growth of ribosomal particles that the lower the Mg^{2+} concentration, the thicker the crystals²⁶⁾. Consequently, crystals from 50S subunits from *H. marismortui*, grown spontaneously under the lowest Mg^{2+} concentration possible, were transferred as seed crystals to solutions with even a lower Mg^{2+} concentration. As a result, after about two weeks well ordered and relatively thick crystals of about $0.6 \times 0.6 \times 0.2$ mm were formed (Fig. 7) that diffracted to about 6 \AA ²⁷⁾.

3 Crystallographic Data Collection — Recent Developments

Only from 1985 onwards could we seriously consider crystallographic data collection. In fact, several full sets of oscillation films have since been exposed on the rotation camera; however, they have tended to become outdated in view of new developments in the crystallization techniques or by other experimental improvements.

3.1 *Bacillus Stearothermophilus*

It initially seemed most promising to use the abovementioned crystal form of 50S subunits of *B. stearothermophilus* grown directly in capillaries. These crystals may now reach a length of 2.0 mm and a cross-section of 0.4 mm, and are loosely packed in an orthorhombic unit cell of $350 \times 670 \times 910 \text{ \AA}$ ²¹⁾. Fresh crystals diffract to 10–13 \AA resolution. However, the higher resolution reflexions decay within 5 to 10 minutes.

Hundreds of crystals were exposed in several synchrotron beam time periods, bearing in mind that there was little chance to solve the inherent problem of how to produce derivative crystals. It was a relief though, that 50S particles from a mutant of *B. stearothermophilus* lacking protein L11 could be crystallized isomorphously²⁸⁾, which might serve as a low resolution deficiency derivative.

3.2 *Halobacterium Marismortui*

Seeded crystals grow in the orthorhombic space group $C222_1$ and diffract to a resolution of up to 6 Å (Fig. 8). They have relatively small, densely packed unit cells of 215*300*590 Å, in contrast to the “open” structure and the large unit cells of the

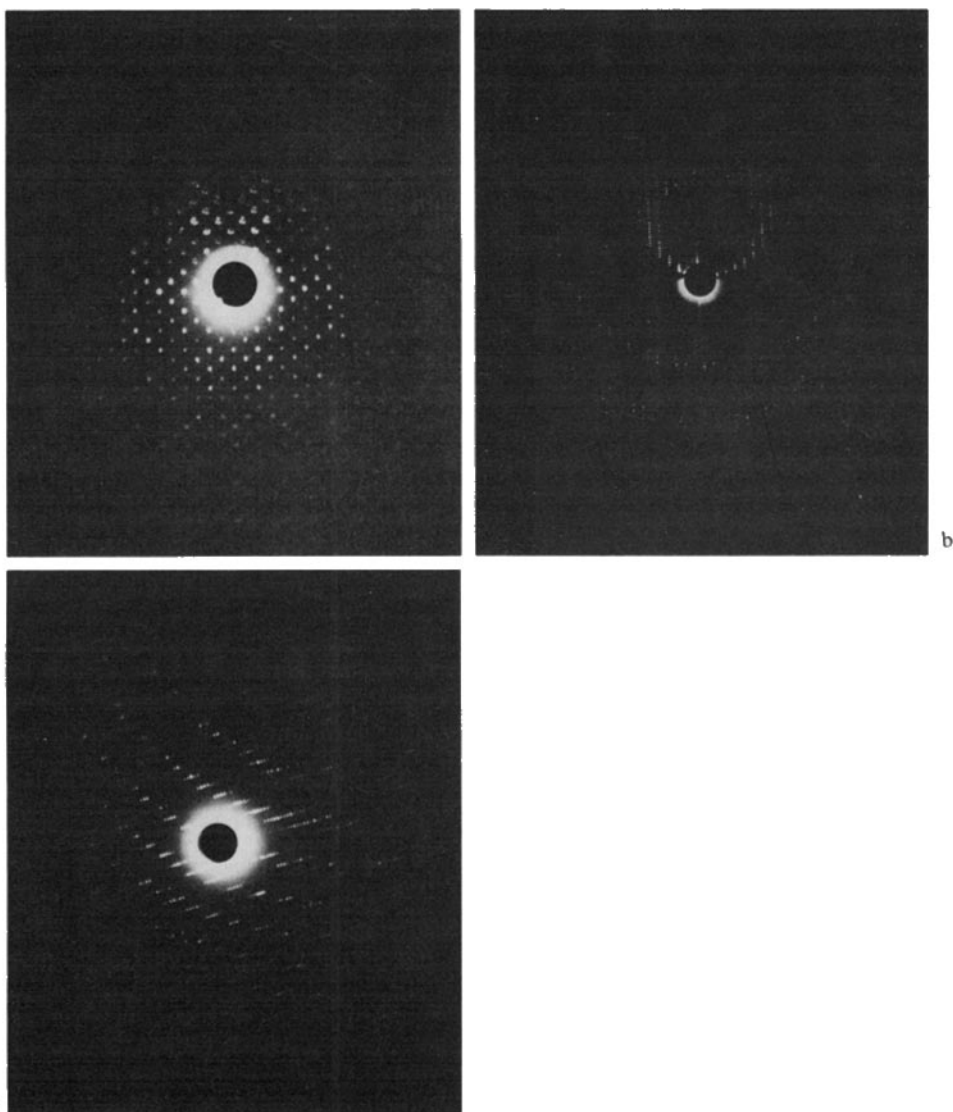


Fig. 8a-c. 1° rotation photographs of *H. marismortui* 50S crystals at 0 °C and at cryotemperature (obtained at X11/EMBL/DESY and at SSRL/Stanford U.) **a** The $hk0$ -orientation of a nearly perfectly aligned (although split) crystal reveals the mirror symmetry of the C-centred lattice plane. The severe overlap problem in this orientation caused by the large mosaic spread is obvious from this picture. **b** The $0kl$ -orientation shows the extinctions of the twofold screw axis. **c** The best crystals have a Bragg resolution limit of about 6 Å, which decreases to about 9 Å in the course of a hundred exposures

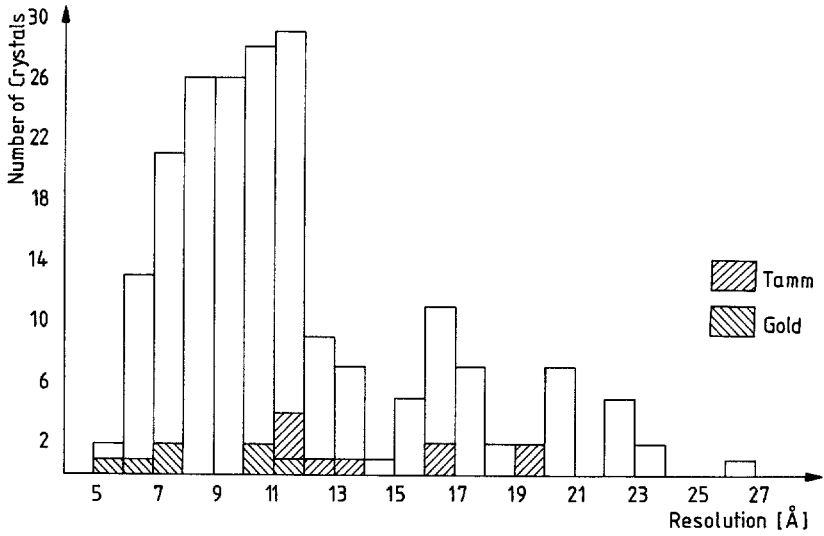


Fig. 9. Approximate Bragg resolution for the first exposure of each of about 200 crystals from *H. marismortui* 50S subunits that were investigated at X11, EMBL/DESY, Hamburg (FRG), in August 1986 at -4° to 19° C. Shading indicates heavy-atom derivative test crystals (undecagold-cluster and tetrakis(acetoxymcuri)methane (TAMM); see paragraph 4: Phase Determination)

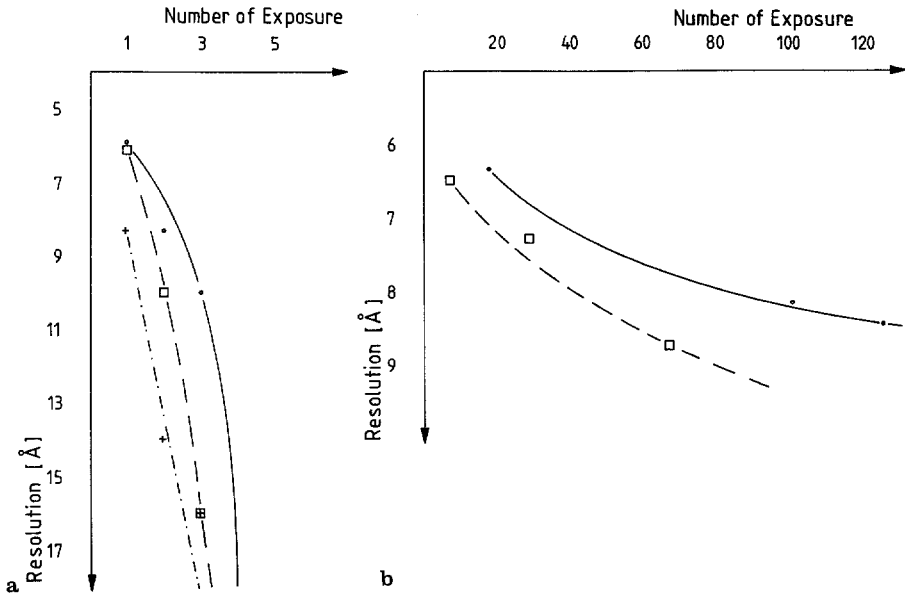


Fig. 10a and b. Decrease of Bragg resolution with time for crystals from *H. marismortui* 50S subunits when irradiated at -4° to 19° C (left) and at cryotemperature (right). (Different symbols represent different crystals.)

crystals from 50S subunits of *B. stearotherophilus*. Up to 10 photographs can be taken from an individual crystal between $-2\text{ }^{\circ}\text{C}$ and $19\text{ }^{\circ}\text{C}$ but the high resolution reflexions appear only on the first 1–3 X-ray photographs. Hence, over 260 crystals had to be irradiated in order to obtain a (supposedly) complete set of film data.

Crystals were aligned only visually to avoid the loss of precious reflexions in the higher resolution range in the course of setting photographs. None of the data films happened to show the orthorhombic symmetry, thus our preliminary report specified the approximate cell constants for the primitive monoclinic cell $P2_1^{27}$. Fig. 9 shows the statistical distribution of approximate Bragg resolution found for the first film from each crystal, Fig. 10a displays the quick loss in resolution as a function of the exposure time/film number. In order to average out the resolution decay during each exposure, the camera rotation axis was oscillated 10 times per photograph.

However, most crystals have a very large mosaic spread of up to 3° even in the first picture. This is indeed larger than the permissible rotation range at our current resolution. Hence there is a severe problem with overlap, in particular when the long 590 \AA axis is in the direction of the X-ray beam. What is worse, for many crystals we are left with no fully recorded reflexions to scale the partial intensities (“post refinement”, ²⁹). These problems, taken together with the short lifetime render even a joint refinement of all the three axes of individual crystals nearly impossible.

All this led to the question whether much lower temperatures might help to increase the lifetime of the crystals in the X-ray beam. We were introduced to cryotemperature crystallography, and learned how to embed the crystals in inert oil or similar materials before deep-freezing ³⁰ instead of keeping them in capillaries. With this technique at least some crystals with Bragg resolution of about 6 \AA could be transferred to liquid nitrogen temperature and would “live” in the synchrotron beam for many hours or even days (Fig. 10b). Figure 11 displays the initial Bragg resolution of those crystals that survived the procedure. As might be expected, the mosaic spread did not become smaller in the course of all this treatment, but it did not become much worse either.

In order to extract the crystals from their solution, tiny spatulas were constructed from very thin glass “saucers” glued to glass rods, which could be mounted on the

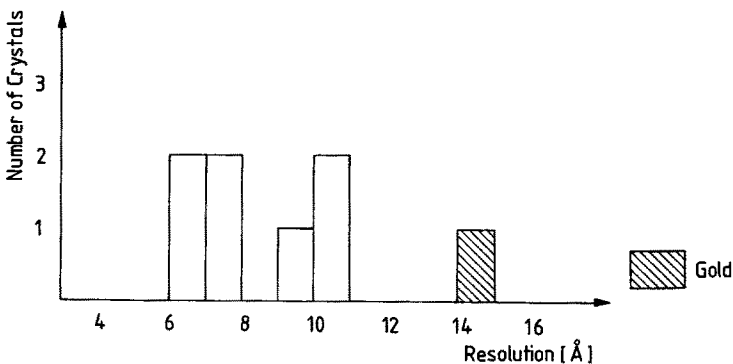


Fig 11. Approximate Bragg resolution for the first exposure of each of eight crystals (incl. one gold derivative) from *H. marismortui* 50S subunits that were investigated at SSRL beam-line 7-1 (Stanford University, Ca., USA) at cryotemperature

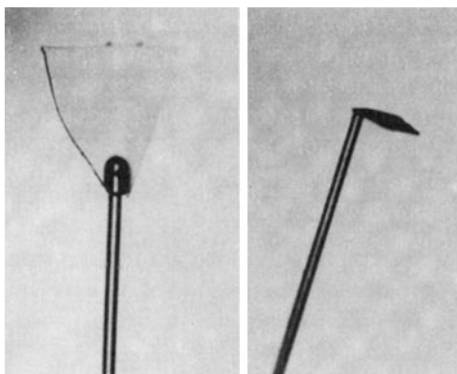


Fig. 12. Views of flat (left) and perpendicular (right) glass spatulas constructed for crystallographic studies of plate-like crystals from *Halobacterium marismortui* 50S subunits at cryotemperature. The long c-axis (i.e. the shortest crystal dimension) will coincide with the spindle axis (and overlap problems will be less severe) when perpendicular spatulas are used

goniometer head in a way familiar to small-molecule crystallographers. The first spatulas were flat, causing the same overlap problems as before. Now we have learned to glue the spatulas at different angles (Fig. 12) so as to preorient the crystal plates in directions that minimise the overlap problem.

There was some hope that the successes with cryotemperature methods would make progress less dependent on a high intensity synchrotron beam and that at least preliminary experiments such as the search for isomorphous derivatives would become feasible in our own laboratory. However, experience in the past year has taught us that neither a weaker synchrotron beam nor a rotating anode ever yields a diffraction pattern comparable in Bragg resolution to Figure 8c.

4 Phase Determination

The large size of ribosomal particles is an obstacle for crystallographic studies, but permits direct investigation by electron microscopy. A model (Fig. 13) obtained by three-dimensional image reconstruction of two-dimensional sheets (e.g. ³¹) may be used for gradual phasing of low resolution crystallographic data.

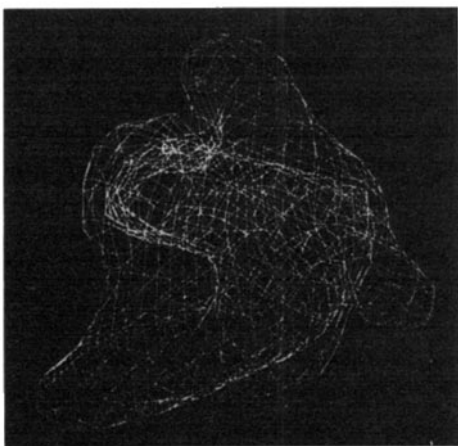


Fig 13. Computer graphics display of the model of the *B. stearothermophilus* 50S subunit reconstructed from 2-dimensional sheets at 30 Å resolution

Heavy-atom derivation of an object as large as a ribosomal particle requires the use of extremely dense and ultraheavy compounds. Examples of such compounds are a) tetrakis(acetoxy-mercuri)methane (TAMM) which was the key heavy atom derivative in the structure determination of nucleosomes³²⁾ and the membrane reaction center³³⁾, and b) an undecagold cluster in which the gold core has a diameter of 8.2 Å (Fig. 14 and in³⁴⁾ and³⁵⁾). Several variations of this cluster, modified with different ligands, have been prepared³⁶⁾. The cluster compounds, in which all the moieties R (Fig. 14) are amine or alcohol, are soluble in the crystallization solution of 50S subunits from *H. marismortui*. Thus, they could be used for soaking. Crystallographic data (to 18 Å resolution) show isomorphous unit cell constants with observable differences in the intensities (Fig. 15).

Because surfaces of ribosomal particles have a variety of potential binding sites for such clusters, attempts are in progress to bind heavy-atoms covalently to a few specific sites on the ribosomal particles prior to crystallization. This may be achieved either by direct interaction of a heavy-atom cluster with chemically active groups such as -SH or the ends of rRNA³⁷⁾ on the intact particles or by covalent attachment of a cluster to natural or tailor-made carriers that bind specifically to ribosomes.

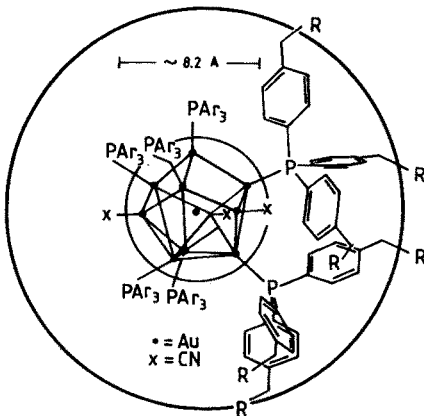


Fig. 14. Semi-schematic presentation of the undecagold cluster depicting the gold core of 8.2 Å diameter, and the arrangement of ligands around it (after⁴³⁾ and literature cited therein)

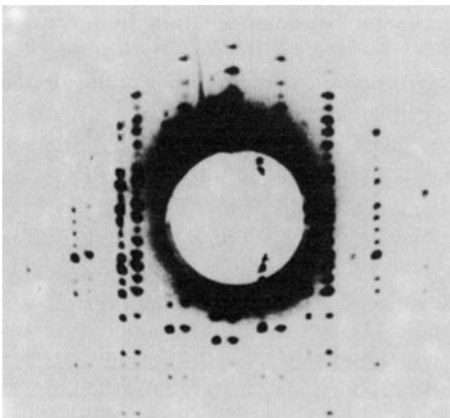


Fig. 15. Superposition of the central reflexion patterns (obtained at SSRL/Stanford U.) of a native and an undecagold derivative crystal (rotation photographs of nearly identical orientations, slightly shifted against each other to facilitate comparison of intensities)

For direct binding to the surfaces of the ribosomes, the following approaches were used: Firstly, free sulfhydryls on the surface of the 50S subunit were located by reacting with radioactive N-ethylmaleimide. The labeled proteins were identified by locating radioactivity in two-dimensional gels. For 50S subunits from *B. stearothermophilus*, the two proteins BL11 and BL13 appear to bind N-ethylmaleimide. For *H. marismortui* a significant portion of the radioactivity was associated with a single protein, tentatively named HL11.

Secondly, the gold cluster described above was prepared in such a way that it could be bound to accessible -SH groups. Since this cluster is rather bulky, its accessibility was increased by the addition of spacers of various lengths to the cluster and to the free -SH groups on the ribosomal particles.

Radioactive labeling of this cluster and neutron activation analysis of the gold enabled us to determine the extent of binding of the cluster to the particles. The results of both analytical methods show that a spacer of minimum length of about 10 Å between the -SH group of a ribosomal protein and the N-atom on the cluster is needed for significant binding. Preliminary experiments indicate that the products of the derivatization reaction with 50S particles can be crystallized.

As mentioned above, such clusters may also be bound to biochemical carriers. Examples of these are antibiotics³⁸⁾, DNA oligomers complementary to exposed single-stranded rRNA regions³⁹⁾ and Fab fragments of antibodies specific to ribosomal proteins. Most of the interactions of these compounds have been characterized biochemically; the crystallographic location of the heavy-atom compounds will thus not only be used for phase determination but will also reveal the specific functional sites on the ribosome. Alternatively, such clusters may be attached to selected sites on isolated ribosomal components; the latter will subsequently be incorporated into particles that lack them. Thus, a mutant of *B. stearothermophilus* that lacks protein BL11 was obtained by growing cells in the presence of thiostrepton at 60 °C⁴⁰⁾. The 50S mutated ribosomal subunits yield sheets and crystals, isomorphous with those of 50S from the wild-type²⁸⁾. This indicates that BL11 is not involved in crystal forces in the native crystals. Furthermore, protein BL11 has only one sulfhydryl group, and binding of N-ethylmaleimide to it does not reduce the biological activity and crystallizability of the particles.

Since protein BL11 is nearly globular⁴¹⁾ its location may be determined in a Patterson map with coefficients of $[F(\text{wild})-F(\text{mutant})]^2$ and may serve, by itself, as a giant heavy-atom derivative. At preliminary stages of structure determination this approach may provide phase information and reveal the location of the lacking protein.

Correspondingly, we have also adopted a procedure for removing several selected proteins from the ribosomal subunits of *B. stearothermophilus*⁴²⁾. The deleted proteins were, in turn, incorporated into the depleted core particles and the activity and crystallizability of the reconstituted particles were checked. Preliminary studies reconfirm the results obtained with the mutant which lacks protein BL11.

Furthermore, there is a good correlation between recovery of activity and ability to crystallize. Thus, particles lacking protein BL12, which are inactive biologically, could not be crystallized, whereas the reconstituted particles produce crystals isomorphous with the native form.

5 Summary

We have shown that out of fifteen forms of three-dimensional crystals from ribosomal particles, grown so far in our laboratory, some appear suitable for crystallographic data collection when using synchrotron radiation at temperatures between 19 °C and -180 °C: 50S subunits from *H. marismortui*., and from *B. stearothermophilus*, including the -BL11 mutant, and the new crystal forms from *B. stearothermophilus* 50S and *Thermus thermophilus* 30S subunits which have only recently been grown in non-volatile precipitants²²). We also plan to continue research on biochemically modified particles, such as 50S with one tRNA and its nascent polypeptide chain (which have already been crystallized).

All this should eventually lead to a three-dimensional model which, (if not at the atomic level), should show molecular details that may assist in the understanding of the interaction of the ribosome with the variety of other components which cooperate in the biosynthetic process.

6 Acknowledgements

We wish to thank Dr. H. D. Bartunik, K. Wilson, J. Helliwell, M. Papiz, K. Moffat, W. Schildkamp, P. Phizackerley, and E. Merrit, and their respective staff for their support on the synchrotron radiation facilities EMBL/DESY, SRS, CHESS and SSRL.

We are grateful to Drs. H. Hope and C. Kratky who have introduced us to and extensively collaborated on using cryotemperatures, to Drs. F. Frolow and M. A. Saper for their efforts in data collection, to our students K. v. Boehlen and K. Stegen, and to H. Danz, H. S. Gewitz, C. Glotz, Y. Halfon, G. Idan, I. Makowski, J. Müssig, J. Piefke, B. Romberg, and P. Webster for skillful technical assistance.

This work was supported by BMFT (05 180 MP BO), NIH (GM 34360) and Minerva research grants.

7 References

1. Chambliss, G., Craven, G. R., Davies, J., Davies, K., Kahan, L., Nomura, M. (eds): *Ribosomes: Structure, Function, and Genetics*. Baltimore, Univers. Park Press 1980
2. Wittmann, H. G.: *Ann. Rev. Biochem.* *51*, 155 (1982)
3. Wittmann, H. G.: *ibid.* *52*, 35 (1983)
4. Liljas, A.: *Progr. Biophys. Mol. Biol.* *40*, 161 (1982)
5. Hardesty, B., Kramer, G. (Eds.): *Structure, Function, and Genetics of Ribosomes*, Springer-Verlag, Heidelberg and New York 1986
6. Byers, B.: *J. Mol. Biol.* *26*, 155 (1967)
7. Unwin, P. N. T.: *Nature* *269*, 118 (1977)
8. Milligan, R. A., Unwin, P. N. T.: *ibid.* *319*, 693 (1986)
9. Yonath, A. E., Müssig, J., Tesche, B., Lorenz, S., Erdmann, V. A., Wittmann, H. G.: *Biochem. Intern.* *1*, 428 (1980)
10. Yonath, A., Wittmann, H. G.: *Biophys. Chem.* *29*, 17-29 (1988)
11. Trakhanov, S. D., Yusupov, M. M., Agalarov, S. C., Garber, M. B., Ryazantsev, S. N., Tischenko, S. V., Shirokov, V. A.: *FEBS Letters* *220*, 319 (1987)

12. Wittmann, H. G., Müssig, J., Piefke, J., Gewitz, H. S., Rheinberger, H. J., Yonath, A.: *ibid.* 146, 217 (1982)
13. Zubay, G., Wilkins, M. H. F.: *J. Mol. Biol.* 2, 105 (1960)
14. Klug, A., Holmes, K. C., Finch, J. T.: *ibid.* 3, 87 (1961)
15. Langridge, R., Holmes, K. C.: *ibid.* 5, 611 (1962)
16. Yonath, A., Khavitch, G., Tesche, B., Müssig, J., Lorenz, S., Erdmann, V. A., Wittmann, H. G.: *Biochem. Intern.* 5, 629 (1982)
17. Yonath, A., Müssig, J., Wittmann, H. G.: *J. Cell. Biochem.* 19, 145 (1982)
18. Yonath, A., Tesche, B., Lorenz, S., Müssig, J., Erdmann, V. A., Wittmann, H. G.: *FEBS Letters* 154, 15 (1983)
19. Yonath, A., Piefke, J., Müssig, J., Gewitz, H. S., Wittmann, H. G.: *ibid.* 163, 69 (1983)
20. Yonath, A., Bartunik, H. D., Bartels, K. S., Wittmann, H. G.: *J. Mol. Biol.* 177, 201 (1984)
21. Yonath, A., Saper, M. A., Makowski, I., Müssig, J., Piefke, J., Bartunik, H. D., Bartels, K. S., Wittmann, H. G.: *ibid.* 187, 633 (1986)
22. Glotz, C., Müssig, J., Gewitz, H. S., Makowski, I., Arad, T., Yonath, A., Wittmann, H. G.: *Biochem. Intern.* 15, 953 (1987)
23. Bartunik, H. D., Gehrmann, T., Robrahn, B.: *J. Appl. Crystallogr.* 17, 120 (1984)
24. Shevack, A., Gewitz, H. S., Hennemann, B., Yonath, A., Wittmann, H. G.: *FEBS Letters* 184, 68 (1985)
25. Shoham, M., Müssig, J., Shevack, A., Arad, T., Wittmann, H. G., Yonath, A.: *ibid.* 208, 321 (1986)
26. Arad, T., Leonard, K. R., Wittmann, H. G., Yonath, A.: *The EMBO Journal* 3, 127 (1984)
27. Makowski, I., Frolow, F., Saper, M. A., Shoham, M., Wittmann, H. G., Yonath, A.: *J. Mol. Biol.* 193, 819 (1987)
28. Yonath, A., Saper, M. A., Frolow, F., Makowski, I., Wittmann, H. G.: *ibid.* 192, 161 (1986)
29. Rossmann, M. G., Leslie, A. G. W., Abdel-Meguid, S. S., Tsukihara, T.: *J. Appl. Crystallogr.* 12, 570 (1979)
30. Hope, H.: *Acta Crystallogr.* B44, 22–26 (1988)
31. Yonath, A., Leonard, K. R., Wittmann, H. G.: *Science* 236, 813 (1987)
32. Richmond, T., Finch, J. T., Rushton, B., Rhodes, D., Klug, A.: *Nature* 311, 533 (1984)
33. Deisenhofer, J., Epp, O., Mikki, K., Huber, R., Michel, H.: *J. Mol. Biol.* 180, 385 (1984)
34. Bellon, P., Manassero, P. M., Sansoni, M.: *J. Chem. Soc. Dalton Trans.*, 1481 (1972)
35. Wall, J. S., Hainfeld, J. F., Barlett, P. A., Singer, S. J.: *Ultramicroscopy* 8, 397 (1982)
36. Weinstein, S., Jahn, W.: private communication
37. Odom Jr., O. W., Robbins, D. R., Lynch, J., Dottavio-Martin, D., Kramer, G., Hardesty, B.: *Biochem.* 19, 5941 (1980)
38. Nierhaus, K. H., Wittmann, H. G.: *Naturwissenschaften* 67, 234 (1980)
39. Hill, W. E., Trappich, B. E., Tassanakajohn, B.: *Probing Ribosomal Structure and Function, in: Structure, Function and Genetics of Ribosomes* (ed.) Hardesty, B. and Kramer, G., p. 233, Springer-Verlag, Heidelberg and New York 1986
40. Schnier, J., Gewitz, H. S., Leighton, B.: to be published
41. Giri, L., Hill, W. E., Wittmann, H. G., Wittmann-Liebold, B.: *Adv. Prot. Chem.* 36, 1 (1984)
42. Gewitz, H. S., Glotz, C., Goischke, P., Romberg, B., Müssig, J., Yonath, A., Wittmann, H. G.: *Biochem. Intern.* 15, 887 (1987)
43. Reardon, J. E., Frey, P. A.: *Biochem.* 23, 3849 (1984)